Thermal Fault-Tolerance in Lithium-ion Battery Cells: A Barrier Function based Input-To-State Safety Framework

Shashank Dhananjay Vyas, Tanushree Roy, and Satadru Dey

Abstract-Ever increasing demand and use of Lithium-ion batteries has made it necessary to put extensive efforts in their safety. While a lot of research is focused on safer battery materials and mechanical designs, developing control-based safety strategies is also a key aspect to enable safety. Most of the existing battery control strategies focus on optimal charging performance, leaving a gap on thermal safety control techniques. Specifically, thermal management of battery cells under thermal faults remains significantly under-explored. In light of this, we propose a fault-tolerant control algorithm which can practically ensure safety of Li-ion batteries in presence of thermal anomalies. In this algorithm, we formulate a control law which guarantees both the thermal safety and stability of Li-ion batteries. Specifically, we combine lumped parameter thermal model and Ordinary Differential Equation (ODE)based practical input-to-state safety technique to formulate the thermal control problem. Subsequently, we utilize control barrier function and linear stability criteria to design the controller gains. Finally, we present simulation case studies to validate the efficacy of the proposed control algorithm.

I. INTRODUCTION

In recent years, owing to a booming Li-ion battery industry, considerable scope of improvement lies in the area of safety of Li-ion batteries. Existing battery control problems typically consider charging control [1], constraint management [2], [3], charge and thermal balancing [4]. Some thermal management approaches have also been presented [5]–[8]. However, these thermal control approaches do not consider control in the presence of battery faults. To impact battery safety, it is essential to consider the presence of battery faults in the design phase of the control algorithms. Along this line, some works have been reported that consider sensor fault-tolerant control of batteries [9]. However, fault-tolerance under internal thermal faults has been significantly under-explored. In [10], an active fault tolerant control scheme for internal thermal faults has been proposed. However it has potential drawbacks which include [11]: (i) A real-time fault detector and estimator is needed. (ii) The effectiveness depends on accuracy of fault detector and estimator since any inaccuracy may induce delay in fault accommodation [11]. To avoid these drawbacks, we propose a passive fault-tolerant control algorithm leveraging ODEbased practical input-to-state safety technique.

*This work was supported by National Science Foundation under Grant No. 2050315. The opinions, findings, and conclusions or recommendations expressed are those of the author(s) and do not necessarily reflect the views of the National Science Foundation.

S. Vyas, T. Roy, and S. Dey are with the Department of Mechanical Engineering, The Pennsylvania State University, University Park, Pennsylvania 16802, USA. {sbv5192,tbr5281,skd5685}@psu.edu.

The notion of input-to-state safety for ODE systems was introduced in [12] and was analyzed in [13]–[15] using Barrier function based approach. In [16] and [17], the notion of practical input-to-state safety was presented augmenting on the original notion. In this work, we adopt the approach presented in [16]. Specifically, the goal is to ensure that a metric, which computes the distance of the system states from a pre-defined unsafe region, is lower bounded by a combination of several terms related to initial condition and inputs [16]. In our work, we adopt this technique to design the control algorithm such that the temperature states never enter the unsafe region even under the presence of faults.

Keeping in mind the research gaps mentioned earlier, the main contribution of this paper is a passive fault-tolerant control algorithm to enable safety under thermal faults. In this algorithm, we formulate a control law which guarantees both the thermal safety and stability by combining lumped parameter battery cell thermal model and ODE-based practical input-to-state safety technique. Particularly, we design a control gain matrix such that battery temperatures get stabilized while remaining under the safe operating limits. In order to arrive at such design, a Barrier function based approach is used to devise the conditions to be satisfied by the control gain matrix such that temperatures never reach values beyond the safe range. Then the closed loop linear stability constraint is applied to the gains obtained from earlier conditions to keep the temperatures stable in the safe region.

A related work is presented in [18] where a Partial Differential Equation (PDE)-based input-to-state safety technique is applied to a battery module under thermal anomalies. The differences between the current work and [18] are as follows. (i) In [18], battery modules are considered which have large spatial temperature variation. Whereas the current work considers battery cells which do not have significant spatial temperature variation, so we utilize a lumped thermal model eliminating the need for complicated PDE analyses. (ii) Three sensors are considered in [18] for measurements, whereas only two sensors are considered in current work, thus achieving safety with limited sensing, and further reducing the implementation cost. (iii) We consider the coolant dynamics in our analysis which is not accounted for in [18].

The organization of the rest of the paper is as follows: Section II describes the thermal model of the battery considered and discusses the problem statement. Section III explains the practical input-to-state safety based thermal control algorithm. Section IV shows the results from the simulation case studies. Section V concludes the paper.

II. PROBLEM STATEMENT: THERMAL FAULT-TOLERANCE IN LI-ION BATTERY CELLS

For our purpose, we adopt a lumped parameter nominal thermal model for cylindrical battery cells from [19], [20], and subsequently model the faults as unknown additive terms acting on the core and surface of the battery cell [21]. The resulting equations are:

$$\dot{T}_1(t) = -\frac{T_1(t) - T_2(t)}{R_1 C_1} + \frac{\dot{Q}(t)}{C_1} + \frac{f_1(t)}{C_1},\tag{1}$$

$$\dot{T}_1(t) = -\frac{T_1(t) - T_2(t)}{R_1 C_1} + \frac{\dot{Q}(t)}{C_1} + \frac{f_1(t)}{C_1}, \qquad (1)$$

$$\dot{T}_2(t) = -\frac{T_2(t) - T_1(t)}{R_1 C_2} - \frac{T_2(t) - T_\infty(t)}{R_2 C_2} + \frac{f_2(t)}{C_2}, \quad (2)$$

where T_1 and T_2 are the battery core and surface temperatures, respectively; T_{∞} is the ambient temperature which is the temperature of cooling system here; R_1 and R_2 are the thermal resistances of the battery between its core and surface, and surface and ambient, respectively; C_1 and C_2 are the heat capacities of the battery material at core and at surface, respectively; $f_1(t)$ and $f_2(t)$ are the thermal faults which may occur due to unwanted chemical reactions, abnormal heat generation inside the battery or mechanical disruptions [22]–[24]; and Q is the internal heat generation given by [25]:

$$\dot{Q}(t) = I(t) \left(V_{ocv}(SOC) - V_t(t) - T_1(t) \frac{d(OCV)}{dT} \right),$$

where I is current through the battery; V_{ocv} is the open circuit voltage of the battery which is a function of state of charge (SOC) of the battery cell, $\frac{dOCV}{dT}$ is the entropic heat coefficient; and V_t is the terminal voltage of the battery. Rearranging the terms of (3), we write:

$$\dot{Q}(t) = R_s u_1^2(t) - \alpha I(t) T_1(t), \tag{4}$$

where $R_s u_1^2(t)$ is the approximation of the term $I(t)(V_{ocv}(SOC) - V_t(t))$ with $u_1(t) = I(t)$; and $\alpha = \frac{d(OCV)}{dT}$. Next, the cooling system dynamics is considered as [21]:

$$\dot{T}_{\infty}(t) = -\frac{T_{\infty}(t) - T_{2}(t)}{R_{2}C_{\infty}} - \frac{\dot{Q}_{c}(t)}{C_{\infty}},$$
(5)

where C_{∞} is the heat capacity of the cooling system and Q_c is the cooling system power. This model is based on liquid cooling where we control \dot{Q}_c by changing the flow rate of the coolant.

Next, we construct the state-space model of the battery temperature dynamics (1)-(5) which is as follows:

$$\dot{T}(t) = (A_0 + A_1(I))T(t)
+ B_1 R_s u_1^2(t) + B_2 u_2(t) + F\Delta(t), \quad (6)$$

where
$$A_0 = \begin{bmatrix} -\frac{1}{C_1 R_1} & \frac{1}{C_1 R_1} & 0\\ \frac{1}{C_2 R_1} & -\frac{1}{C_2} (\frac{1}{R_1} + \frac{1}{R_2}) & \frac{1}{C_2 R_2}\\ 0 & \frac{1}{C_\infty R_2} & -\frac{1}{C_\infty R_2} \end{bmatrix}$$
, (7a)
$$A_1(I) = \begin{bmatrix} -\frac{\alpha I}{C_1} & 0 & 0\\ 0 & 0 & 0 \end{bmatrix}, \quad B_1 = \begin{bmatrix} \frac{1}{C_1}\\ 0 \end{bmatrix}, \quad (7b)$$

$$B_2 = \begin{bmatrix} 0 \\ 0 \\ -\frac{1}{C_{co}} \end{bmatrix}, \quad F = \begin{bmatrix} \frac{1}{C_1} & 0 \\ 0 & \frac{1}{C_2} \\ 0 & 0 \end{bmatrix}, \tag{7c}$$

and $T(t) = \begin{bmatrix} T_1(t) & T_2(t) & T_{\infty}(t) \end{bmatrix}'$ is the state vector; $u_2 = \dot{Q}_c$ is the control input; and $\Delta(t) = \begin{bmatrix} f_1(t) & f_2(t) \end{bmatrix}$ is the fault vector. A schematic of the battery thermal model along with cooling system is shown in Fig. 1.

Remark 1. In this work, we assume that the surface temperature (T_2) and the coolant temperature (T_∞) are measured in real-time. Accordingly, the output equation corresponding to the state-space model is

$$y = \begin{bmatrix} T_2 \\ T_{\infty} \end{bmatrix} = CT$$
, where $C = \begin{bmatrix} 0 & 1 & 0 \\ 0 & 0 & 1 \end{bmatrix}$. (8)

Remark 2. We consider only cooling power (\dot{Q}_c) as the control input and not the current (I). Although the battery current is typically measured and hence, a known variable to the controller, oftentimes the current is determined to satisfy the power demand from the battery. For example, in vehicles, current drawn depends on the action of the driver. Under such scenarios, the current is not manipulated by the thermal control unit and cooling power remains the only control variable.

To this end, the control objective is to ensure thermal safety of the battery under faults. In order to achieve the same, we establish two control objectives for the battery under the fault:

- To ensure the temperatures do not reach any value in a pre-defined unsafe operating range during its operation, even in the presence of faults.
- To keep the closed-loop temperature dynamics stable.

We assume that the cooling power is sufficient to achieve the control objectives. A schematic of the battery cell and the control system is shown in Fig. 1.

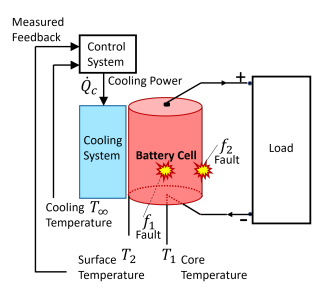


Fig. 1. Schematic of battery cell and control system.

To attain the above control objectives, we aim to design a feedback control law of the following form:

$$u_2 = -KC(T - T_{ref}), (9)$$

 $A_1(I) = \begin{bmatrix} -\frac{\alpha I}{C_1} & 0 & 0 \\ 0 & 0 & 0 \\ 0 & 0 & 0 \end{bmatrix}, \quad B_1 = \begin{bmatrix} \frac{1}{C_1} \\ 0 \\ 0 \end{bmatrix}, \qquad \text{where } \mathbf{A} = \begin{bmatrix} \mathbf{A}_2 & \mathbf{A}_3 \end{bmatrix} \text{ is the connect games}$ where $\mathbf{A} = \begin{bmatrix} \mathbf{A}_2 & \mathbf{A}_3 \end{bmatrix} \text{ is the connect games}$ as the reference steady state temperature vector such that $T \to T_{ref}$ as $t \to \infty$. where $K = \begin{bmatrix} K_2 & K_3 \end{bmatrix}$ is the control gain matrix. We take

Next, we apply a change of variables given by $\xi = T - T_{ref}$ in (6), and subsequently use (9) to obtain:

$$\dot{\xi}(t) = (P + A_1(I))\xi(t) + B_1 R_s u_1^2(t) + (A_0 + A_1(I))T_{ref} + F\Delta(t), \quad (10)$$

where $P = A_0 - B_2 KC$. In the next section, we discuss the details of the control gain design.

III. PRACTICAL INPUT-TO-STATE SAFETY BASED THERMAL CONTROL ALGORITHM

Our goal is to design the control gain K such that the two aforementioned control objectives are satisfied. To this end, we formulate the first control objective following the notion of practical input-to-state safety. Subsequently, the second control objective will be satisfied by ensuring that eigenvalues of the closed-loop temperature system have negative real parts. Next, we discuss the notion of practical input-to-state safety in detail.

A. Practical Input-To-State Safety

The notion of input-to-state safety essentially formulates inequality type conditions to ensure the system states are within safe operating region [16]. Adopting the definition presented in [16], the system (10) is considered to be practically input-to-state safe if the following condition holds: $(|\xi|_{\mathbb{D}}) \geq \alpha_1(|\xi(0)|_{\mathbb{D}}) - \alpha_2(||\delta||) - \alpha_3, \forall t \text{ where } |\xi|_{\mathbb{D}} \text{ is the safety distance between the system state } \xi \text{ and a pre-defined unsafe set; } \delta \text{ captures the effects of inputs } u_1 \text{ and } \Delta; \alpha_1, \alpha_2 \text{ are class } \mathcal{KK} \text{ functions [16], and } \alpha_3 \text{ is a positive constant.}$

Such practical input-to-state safety can be equivalently characterized using Barrier functions [16]. Under this characterization, our objective is to find a Barrier function $\mathbb{B} \colon \mathbb{R}^3 \to \mathbb{R}$, with respect to the system (10), which satisfies the following inequalities [16], [18]:

$$-c_1|\xi|_{\mathbb{D}}^2 - \kappa_1 \leqslant \mathbb{B}(\xi) \leqslant -c_2|\xi|_{\mathbb{D}}^2, \tag{11}$$

$$\dot{\mathbb{B}}(\xi) \leqslant -c_3 |\xi|_{\mathbb{D}}^2 + c_4 |u_1|^2 + c_5 ||\Delta||^2 + \kappa_2, \tag{12}$$

where $c_i>0$, i=1,2,3,4,5; $\kappa_i\geqslant 0$, i=1,2, $\|.\|$ indicates the 2-norm. These conditions (11)-(12) implies that the system is practically input-to-state safe with respect to the unsafe set $\mathbb D$. The parameters κ_1 and κ_2 capture the effect of practical considerations in the design.

Remark 3. Note that since the conditions on control gains are dependent on Barrier function, as is evident in the next subsection, the form of Barrier function chosen naturally affects the design. To allow a quadratic form of Barrier function for design, κ_1 ensures that $\mathbb{B}(\xi)$ can be lower bounded on the boundary of unsafe region since $|\xi|_{\mathbb{D}} = 0$ on the boundary [16]. Moreover, the effect of other system and design parameters such as the reference state values and the maximum allowable state values are captured in the parameter κ_2 .

Remark 4. Note that the conditions (11)-(12) are adopted from [16] but slightly modified to suit our problem statement. In the formulation given in [16], only κ_1 is used to characterize the uncertainties in the model. In [18], the parameter

 κ_2 is included in addition to κ_1 to further capture these aforementioned practical aspects of uncertainties. Inclusion of κ_2 provides us additional design freedom. Here, we follow the conditions formulated in [18].

B. Control Design Process

In order to apply the practical input-to-state safety technique, we first focus on defining an unsafe set. Note that the control goal is to be away from the unsafe set while not to deviate too far from the reference temperature $T_{ref} = [T_{1,ref} \ T_{2,ref} \ T_{\infty,ref}]'$. We define upper bounds of the temperature states as \overline{T}_1 , \overline{T}_2 , and \overline{T}_3 where $T_{1,ref} < \overline{T}_1$, $T_{2,ref} < \overline{T}_2$, and $T_{\infty,ref} < \overline{T}_3$. If the temperatures rise beyond these bounds, it will be considered unsafe condition. Based on these bounds, we define the following unsafe set:

$$\mathbb{D} = \{ a = [a_1 \ a_2 \ a_3]' : (a_1^2 + a_2^2 + a_3^2) > \mathcal{M}^2 \}, \tag{13}$$

where $\mathcal{M} := \min(\overline{T}_1 - T_{1,ref}, \overline{T}_2 - T_{2,ref}, \overline{T}_{\infty} - T_{3,ref})$. Next, we define a metric for the distance of the states ξ with respect to the unsafe set \mathbb{D} as follows:

$$|\xi|_{\mathbb{D}} = \inf_{a \in \mathbb{D}} \|\xi - a\|, \qquad (14)$$

where \mathbb{D} is given by (13). Qualitatively, $|\xi|_{\mathbb{D}}$, which is the 2-norm of $(\xi - a)$, $\forall a \in \mathbb{D}$, represents the minimum distance of the state ξ from the unsafe set \mathbb{D} . This essentially implies

$$|\xi|_{\mathbb{D}} = \|\xi - \xi_m\|, \quad \forall \xi \in \mathbb{S} = \mathbb{D}^C, \tag{15}$$

where \mathbb{S} is the safe set, that is, the complement of the unsafe set \mathbb{D} , and $\xi_m = \left[\xi_{1m} \ \xi_{2m} \ \xi_{3m}\right]'$ represents any point on the boundary of \mathbb{S} i.e. $\|\xi_m\| = \mathcal{M}$. A visual representation of the safe and unsafe regions are shown in Fig. 2.

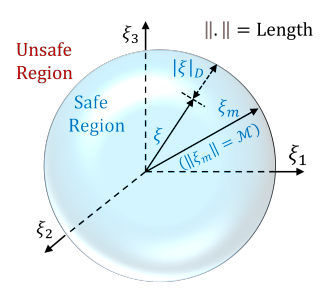


Fig. 2. Visual representation of safe and unsafe regions.

Next, we choose the following Barrier function candidate:

$$\mathbb{B}(\xi) = \|\xi\|^2 - \mathcal{M}^2,\tag{16}$$

where \mathcal{M} is defined after (13).

In order to obtain the left-hand side inequality of (11), we note from the definition (13) that $\forall \xi \in \mathbb{S}$, $\|\xi\| \leq \mathcal{M}$. Now applying triangle inequality to (15) for safe state ξ , we obtain,

$$|\xi|_{\mathbb{D}} \le ||\xi|| + ||\xi_m|| = ||\xi|| + \mathcal{M} \le 2\mathcal{M},$$
 (17)

which further implies $-\frac{1}{4}|\xi|_{\mathbb{D}}^{2}\geqslant -\mathcal{M}^{2}$. In other words, we can find a $\kappa_{1}>0$ such that $-\frac{1}{4}|\xi|_{\mathbb{D}}^{2}-\kappa_{1}=-\mathcal{M}^{2}$. Also, from (16), we can obtain $-\mathcal{M}^{2}\leqslant\mathbb{B}(\xi)$ which yields,

$$-c_1|\xi|_{\mathbb{D}}^2 - \kappa_1 \leqslant \mathbb{B}(\xi), \tag{18}$$

where $c_1 = \frac{1}{4}$. This provides us with the left-hand side inequality of (11).

Next to obtain the right-hand side inequality of (11), we rearrange the terms in (16) to obtain, $\mathbb{B}(\xi) = -(\mathcal{M} - \|\xi\|)^2 - 2\|\xi\| (\mathcal{M} - \|\xi\|)$. Since $\|\xi\| < \mathcal{M}$, it can be seen that $\mathbb{B}(\xi) \leq -(\mathcal{M} - \|\xi\|)^2$. From Fig. 2, it is evident that $|\xi|_{\mathbb{D}} = (\mathcal{M} - \|\xi\|)$. This implies that,

$$\mathbb{B}(\xi) \leqslant -c_2 |\xi|_{\mathbb{D}}^2,\tag{19}$$

where $c_2 = 1$. This provides us with the right-hand side inequality of (11).

Next, we find the condition for which (12) is satisfied. Noting $\|\xi\|^2 = \xi' \xi$, we rewrite (16) as $\mathbb{B}(\xi) = \xi' \xi - \mathcal{M}^2$. Differentiation of which yields $\dot{\mathbb{B}}(\xi) = 2\xi' \dot{\xi}$ which can be written as $\dot{\mathbb{B}}(\xi) = 2(\xi - \xi_m + \xi_m)' \dot{\xi}$ and further substituting $\dot{\xi}$ from (10), we obtain,

$$\dot{\mathbb{B}} = V_0 + V_1 + V_2 + V_3 + V_4 + V_5, \tag{20}$$

where

$$V_0 = (\xi - \xi_m)' P(\xi - \xi_m) + (\xi - \xi_m)' (2P\xi_m + PT_{ref}),$$
(21)

$$V_{1} = -\frac{\alpha(\xi_{1} - \xi_{1m})^{2} u_{1}}{C_{1}} + \frac{R_{s}(\xi_{1} - \xi_{1m}) u_{1}^{2}}{C_{1}} - \frac{2\alpha(\xi_{1m} + \frac{T_{1,ref}}{2})(\xi_{1} - \xi_{1m}) u_{1}}{C_{1}},$$
(22)

$$V_2 = -\frac{\alpha \xi_{1m} (\xi_{1m} + T_{1,ref}) u_1}{C_1} + \frac{R_s \xi_{1m} u_1^2}{C_1},$$
 (23)

$$V_3 = \frac{(\xi_1 - \xi_{1m})f_1}{C_1} + \frac{(\xi_2 - \xi_{2m})f_2}{C_2},\tag{24}$$

$$V_4 = \frac{\xi_{1m} f_1}{C_1} + \frac{\xi_{2m} f_2}{C_2},\tag{25}$$

$$V_{5} = \xi_{m}^{'} P \xi_{m} + \xi_{m}^{'} P T_{ref}. \tag{26}$$

Next, we make use of the Holder's and then Young's inequality of the form

$$xy \le \|x\| \|y\| \le \frac{\bar{\gamma}}{2} \|x\|^2 + \frac{1}{2\bar{\gamma}} \|y\|^2, \ \bar{\gamma} > 0,$$
 (27)

on (21) through (26). Furthermore, denoting $(\xi - \xi_m)$ by $\hat{\xi}$; $(\xi_1 - \xi_{1m})$ by $\hat{\xi}_1$; $(\xi_2 - \xi_{2m})$ by $\hat{\xi}_2$, we obtain the following upper bounds from (21)-(26):

$$V_{0} \leqslant \hat{\xi}' P \hat{\xi} + \gamma_{1} \left\| \hat{\xi} \right\|^{2} + \frac{\left\| 2P \xi_{m} + PT_{ref} \right\|^{2}}{4\gamma_{1}},$$

$$V_{1} \leqslant \alpha \hat{\xi}_{1}^{2} + \gamma_{2} u_{1}^{2} + \frac{1}{4\gamma_{2} C_{1}^{2}} + \gamma_{3} \hat{\xi}_{1}^{2} + \frac{1}{4\gamma_{3}} + \frac{R_{s}}{C_{1}} u_{1}^{2}$$

$$+ \gamma_{4} \hat{\xi}_{1}^{2} + \frac{\alpha^{2} (2\xi_{1m} + T_{1,ref})^{2}}{4\gamma_{4} C_{1}^{2}} u_{1}^{2},$$

$$(28)$$

$$V_2 \leqslant \gamma_5 u_1^2 + \frac{\alpha^2 \xi_{1m}^2 (\xi_{1m} + T_{1,ref})^2}{4\gamma_5 C_1^2} + \frac{R_s \xi_{1m}}{C_1} u_1^2, \quad (30)$$

$$V_3 \leqslant \gamma_6 \hat{\xi}_1^2 + \frac{1}{4\gamma_6 C_1^2} f_1^2 + \gamma_7 \hat{\xi}_2^2 + \frac{1}{4\gamma_7 C_2^2} f_2^2, \tag{31}$$

$$V_4 \leqslant \gamma_8 f_1^2 + \frac{\xi_{1m}^2}{4\gamma_8 C_1^2} + \gamma_9 f_2^2 + \frac{\xi_{2m}^2}{4\gamma_9 C_2^2},\tag{32}$$

where $\gamma_i > 0$, i = 1, 2, ..., 9. Next, using the fact that $\hat{\xi}_1^2 \le \|\hat{\xi}\|^2$, $f_1^2 \le \|\Delta\|^2$ and $f_2^2 \le \|\Delta\|^2$ in (29), (31), (32), and then using (26)-(32) in (20), we obtain,

$$\dot{\mathbb{B}} \leqslant \hat{\xi}' P \hat{\xi} + \gamma \left\| \hat{\xi} \right\|^2 + c_4 u_1^2 + c_5 \left\| \Delta \right\|^2 + \kappa_2, \quad (33)$$

where $\gamma = \gamma_1 + \alpha + \gamma_3 + \gamma_4 + \gamma_6 + \gamma_7$, and

$$c_4 = \gamma_2 + \frac{R_s}{C_1} + \frac{\alpha^2 (2\xi_{1m} + T_{1,ref})^2}{4\gamma_4 C_1^2} + \gamma_5 + \frac{R_s \xi_{1m}}{C_1},$$
(34)

$$c_{5} = \frac{1}{4\gamma_{6}C_{1}^{2}} + \frac{1}{4\gamma_{7}C_{2}^{2}} + \gamma_{8} + \gamma_{9},$$

$$\kappa_{2} = \frac{\|2P\xi_{m} + PT_{ref}\|^{2}}{4\gamma_{1}} + \frac{1}{4\gamma_{2}C_{1}^{2}} + \frac{1}{4\gamma_{3}}$$

$$+ \frac{\alpha^{2}\xi_{1m}^{2}(\xi_{1m} + T_{1,ref})^{2}}{4\gamma_{5}C_{1}^{2}} + \frac{\xi_{1m}^{2}}{4\gamma_{8}C_{1}^{2}} + \frac{\xi_{2m}^{2}}{4\gamma_{9}C_{2}^{2}}$$

$$+ \xi_{m}^{\prime}P\xi_{m} + \xi_{m}^{\prime}PT_{ref}.$$
 (36)

Noting $\left\|\hat{\xi}\right\|^2 = \hat{\xi}'\hat{\xi}$, we rewrite (33) as,

$$\dot{\mathbb{B}} \leqslant -\hat{\xi}' R \hat{\xi} + c_4 u_1^2 + c_5 \|\Delta\|^2 + \kappa_2, \tag{37}$$

where $R = -(P + \gamma \mathbb{I})$ should be designed to be a positive definite matrix with \mathbb{I} being the 3x3 identity matrix.

Given R > 0, we can write

$$\lambda_{min}(R) \left\| \hat{\xi} \right\|^2 \leqslant \hat{\xi}' R \hat{\xi} \leqslant \lambda_{max}(R) \left\| \hat{\xi} \right\|^2,$$
 (38)

where $\lambda_{min}(R)$ and $\lambda_{max}(R)$ be the minimum and maximum eigenvalues of R respectively. Furthermore, since $\hat{\xi} = (\xi - \xi_m)$ as defined after (27), further using (15) we can write (37) as,

$$\dot{\mathbb{B}} \leqslant -c_3 |\xi|_{\mathbb{D}}^2 + c_4 u_1^2 + c_5 \|\Delta\|^2 + \kappa_2, \tag{39}$$

where $c_3 = \lambda_{min}(R)$.

Remark 5. From the design viewpoint, our goal is to ensure that $R=-(P+\gamma\mathbb{I})$ as defined after (37), should be a positive definite matrix. As $P=A_0-B_2KC$, we find the control gain matrix K such that this condition is satisfied. Since $\gamma_i>0,\ i\in\{1,2,\ldots,9\}$, it can be seen that $c_4>0$ and $c_5>0$ as defined in (34) and (35). To ensure that c_3 defined after (39) is positive, it is sufficient to ensure that R>0. Further ensuring $\kappa_2>0$ provides us with the inequality condition (12). Satisfying these conditions essentially makes the system practically input-to-state stable in the sense of (11)-(12).

Note that the system (10) should also be closed-loop stable, according to the second control objective. Hence, the control gain matrix K should further ensure that the closed loop temperature dynamics is stable, i.e., all the eigenvalues of $(P+A_1(I))$ should have negative real part for the range of possible currents $I_{min} \leq I \leq I_{max}$ where I_{min} and I_{max} are the minimum and maximum values of allowable currents, respectively. Let λ_i , $i \in \{1,2,3\}$ be the eigenvalues of $(P+A_1(I))$, then the stability condition is as follows,

$$real(\lambda_i) < 0, i \in \{1, 2, 3\}, \quad \forall \quad I \in [I_{min}, I_{max}].$$
 (40)

C. Final Design Conditions

In summary, the control design that ensures the practical input-to-state safety inequalities and stability condition, should satisfy the following:

$$-(P + \gamma \mathbb{I}) > 0, \tag{41}$$

$$\kappa_2 > 0, \tag{42}$$

$$real(\lambda_i) < 0, i \in \{1, 2, 3\}, \forall I \in [I_{min}, I_{max}],$$
 (43)

where P, γ and \mathbb{I} are defined after (10), (33) and (37), respectively; κ_2 is given by (36); and λ_i , i=1,2,3 are the eigenvalues of $(P+A_1(I))$. An algorithmic guideline for the control design is given in Algorithm 1.

Algorithm 1: Control Design Guidelines.

```
Input: Parameters and system matrices defined in (1)-(8), unsafe set \mathbb{D} given in (13), reference temperature T_{ref}.
```

Output: Control gain matrix K.

- 1 Define current input range $[I_{min}, I_{max}]$.
- 2 Construct a set \mathbb{K}_s of the control gain matrices where each element satisfies (41) and (42).
- 3 Choose a gain matrix K from the set \mathbb{K}_s .

```
4 for i \leftarrow I_{min} to I_{max} do

5 | Evaluate the eigenvalues \lambda_i of (P+A_1(I)).

6 | if real(\lambda_i) \geq 0 then

7 | Discard the gain matrix K. Go to step 3 and choose another gain matrix from the set \mathbb{K}_s.

8 | else

9 | Return K.

10 | end

11 end
```

IV. CASE STUDIES

In this section we present the simulation results. We have considered a cylindrical battery cell. The thermal parameters are taken from [26], [27]. The value of internal electrical resistance R_s and entropic heat coefficient α are taken to be 0.05Ω and $10^{-4}VK^{-1}$, respectively. The simulation studies are performed in MATLAB 2021a. We have added white Gaussian noise in the measurement signals to mimic real applications. To benchmark the proposed approach, an openloop control with a constant cooling rate of 0.05W is considered for comparison. The simulation studies are performed under a dynamic current profile generated based on the repeated Urban Dynamometer Driving Schedule (UDDS) [10], as shown in Fig. 3. Following the steps shown in Algorithm 1, we have obtained the control gains as $K_2 =$ $1.6887WK^{-1},\ K_3=-3.9391WK^{-1}$ where the values of κ_1 and κ_2 are as, $\kappa_1 = 1875K^2$, $\kappa_2 = 1255.4K^2s^{-1}$. Here, T_{ref} is chosen as $25^{o}C$ for all three temperature states and the unsafe region is considered to be beyond $50^{\circ}C$.

When simulated, the temperatures stay below $40^{\circ}C$ with both, open-loop and proposed control, under no fault till t=1000s. Next, we inject an internal fault f_1 at t=1000s

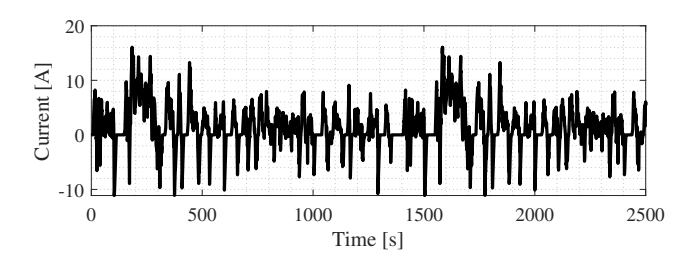


Fig. 3. Applied dynamic current profile based on UDDS velocity profile.

which settles asymptotically to 1.8W. This type of fault represents the anomalous event of abnormal heat generation due to partial (soft) internal short circuit. The heat generation, battery and coolant temperature responses, and cooling power with both, open-loop proposed control, are shown in Fig. 4 under this faulty scenario. From Fig. 4, it can be seen that there is substantial increase in the heat generation Q due to the fault. Owing to this increase in heat generation, the temperatures T_1 , T_2 initially start increasing as seen in Fig. 4. With the open-loop control, the cooling power was not sufficient to remove the heat, hence, the temperatures T_1 , T_2 rise rapidly after the initial increase and eventually enter the unsafe region beyond $50^{\circ}C$. On the other hand, as seen from the bottom plot in Fig. 4, the control power \dot{Q}_c with the proposed control strategy significantly changes to mitigate the effect of the fault. As seen from the T_1 , T_2 plots in Fig. 4, this change in action of the control signal compensates for the increased heat generation and causes the temperatures to stabilize and reach steady state below the unsafe value of $50^{\circ}C$, thus preventing steep rise. For a better visual understanding, a phase-plane plot in the $T_1 - T_2$ space is shown in Fig. 5. It can be seen that with openloop control the temperatures enter the unsafe zone, but the proposed control law keeps them in the safe region.

V. CONCLUSIONS

In this paper, we have proposed a thermal fault-tolerant control algorithm for Lithium-ion batteries. Particularly, the control objective is to maintain the battery temperatures stable in the safe operating range under thermal faults. Specifically, we have used the input-to-state safety approach with the closed loop stability constraint to design the control law. The applicability of the proposed framework is validated through simulation case studies presented in Section IV. It is found that the control gains designed through the algorithm are indeed able to stabilize the temperatures in the safe limits.

REFERENCES

- [1] Qian Lin, Jun Wang, Rui Xiong, Weixiang Shen, and Hongwen He. Towards a smarter battery management system: A critical review on optimal charging methods of lithium ion batteries. *Energy*, 183:220–234, 2019.
- [2] Kandler A Smith, Christopher D Rahn, and Chao-Yang Wang. Model-based electrochemical estimation and constraint management for pulse operation of lithium ion batteries. *IEEE Transactions on Control Systems Technology*, 18(3):654–663, 2009.

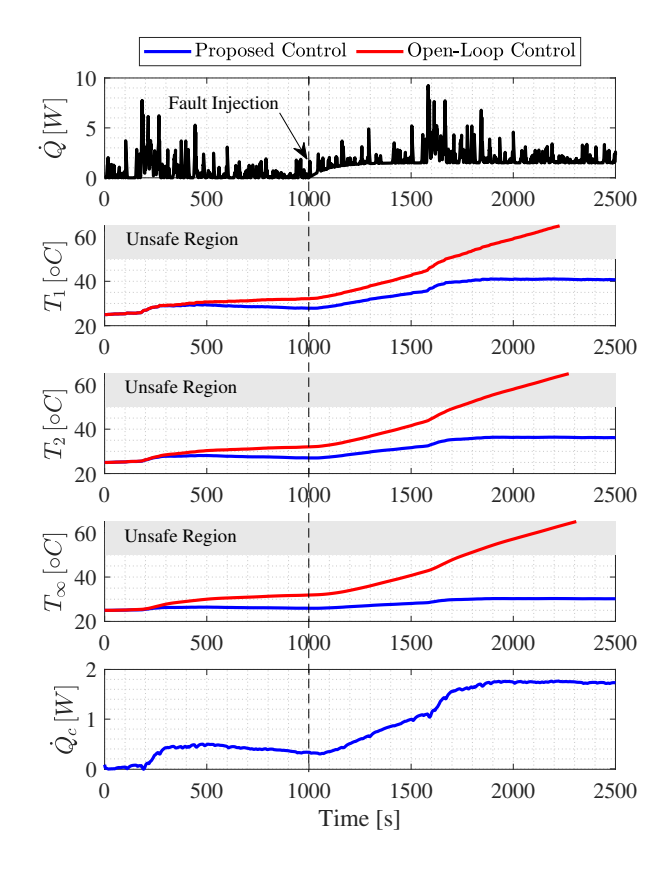


Fig. 4. Heat generation, temperatures, and cooling power under faulty scenario.

- [3] Hector Perez, Niloofar Shahmohammadhamedani, and Scott Moura. Enhanced performance of li-ion batteries via modified reference governors and electrochemical models. *IEEE/ASME Transactions on Mechatronics*, 20(4):1511–1520, 2015.
- [4] Faisal Altaf, Bo Egardt, and Lars Johannesson Mårdh. Load management of modular battery using model predictive control: Thermal and state-of-charge balancing. *IEEE Transactions on Control Systems Technology*, 25(1):47–62, 2016.
- [5] Eugene Kim, Kang G Shin, and Jinkyu Lee. Real-time battery thermal management for electric vehicles. In 2014 ACM/IEEE International Conference on Cyber-Physical Systems (ICCPS), pages 72–83. IEEE, 2014
- [6] Xinran Tao and John Wagner. A thermal management system for the battery pack of a hybrid electric vehicle: modeling and control. Proceedings of the Institution of Mechanical Engineers, Part D: Journal of Automobile Engineering, 230(2):190–201, 2016.
- [7] Yoong Chung and Min Soo Kim. Thermal analysis and pack level design of battery thermal management system with liquid cooling for electric vehicles. *Energy conversion and management*, 196:105–116, 2019.
- [8] Gholamreza Karimi and Xianguo Li. Thermal management of lithiumion batteries for electric vehicles. *International Journal of Energy Research*, 37(1):13–24, 2013.
- [9] Rui Xiong, Quanqing Yu, and Weixiang Shen. Review on sensors fault diagnosis and fault-tolerant techniques for lithium ion batteries in electric vehicles. In 2018 13th IEEE Conference on Industrial Electronics and Applications (ICIEA), pages 406–410. IEEE, 2018.
- [10] Satadru Dey, Ying Shi, Kandler Smith, and Munmun Khanra. Safer batteries via active fault tolerant control. In 2019 American Control Conference (ACC), pages 1561–1566. IEEE, 2019.
- [11] Jin Jiang and Xiang Yu. Fault-tolerant control systems: A comparative study between active and passive approaches. Annual Reviews in control, 36(1):60–72, 2012.
- [12] Peter Wieland and Frank Allgöwer. Constructive safety using control

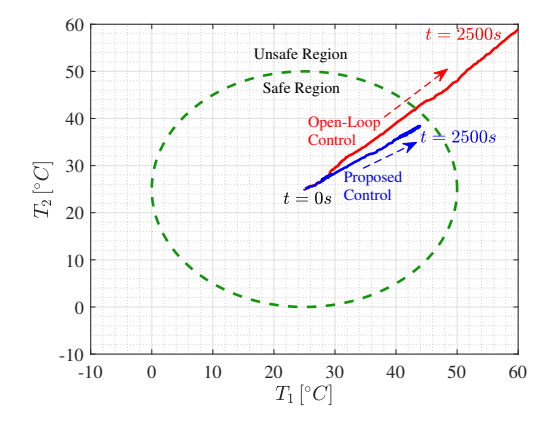


Fig. 5. Phase-plane plot of battery temperatures $T_1 - T_2$ under fault.

- barrier functions. IFAC Proceedings Volumes, 40(12):462-467, 2007.
- [13] Shishir Kolathaya and Aaron D Ames. Input-to-state safety with control barrier functions. *IEEE control systems letters*, 3(1):108–113, 2018
- [14] Xiangru Xu, Paulo Tabuada, Jessy W Grizzle, and Aaron D Ames. Robustness of control barrier functions for safety critical control. IFAC-PapersOnLine, 48(27):54–61, 2015.
- [15] Andrew Taylor, Andrew Singletary, Yisong Yue, and Aaron Ames. Learning for safety-critical control with control barrier functions. In Learning for Dynamics and Control, pages 708–717. PMLR, 2020.
- [16] Muhammad Zakiyullah Romdlony and Bayu Jayawardhana. On the new notion of input-to-state safety. In 2016 IEEE 55th Conference on Decision and Control (CDC), pages 6403–6409. IEEE, 2016.
- [17] Muhammad Zakiyullah Romdlony and Bayu Jayawardhana. Stabilization with guaranteed safety using control lyapunov-barrier function. Automatica, 66:39–47, 2016.
- [18] Tanushree Roy, Ashley Knichel, and Satadru Dey. An input-to-state safety approach to anomaly-resilient parabolic pdes: Application to cyber-physical battery modules. arXiv preprint arXiv:2201.02239, 2022.
- [19] Chanwoo Park and Arun K Jaura. Dynamic thermal model of liion battery for predictive behavior in hybrid and fuel cell vehicles. Technical report, SAE Technical Paper, 2003.
- [20] Xinfan Lin, Hector E Perez, Shankar Mohan, Jason B Siegel, Anna G Stefanopoulou, Yi Ding, and Matthew P Castanier. A lumpedparameter electro-thermal model for cylindrical batteries. *Journal of Power Sources*, 257:1–11, 2014.
- [21] Satadru Dey, Zoleikha Abdollahi Biron, Sagar Tatipamula, Nabarun Das, Sara Mohon, Beshah Ayalew, and Pierluigi Pisu. Model-based real-time thermal fault diagnosis of lithium-ion batteries. *Control Engineering Practice*, 56:37–48, 2016.
- [22] Todd M Bandhauer, Srinivas Garimella, and Thomas F Fuller. A critical review of thermal issues in lithium-ion batteries. *Journal of the Electrochemical Society*, 158(3):R1, 2011.
- [23] Daniel H Doughty and E Peter Roth. A general discussion of li ion battery safety. The Electrochemical Society Interface, 21(2):37, 2012.
- [24] Christopher Hendricks, Nick Williard, Sony Mathew, and Michael Pecht. A failure modes, mechanisms, and effects analysis (fmmea) of lithium-ion batteries. *Journal of Power Sources*, 297:113–120, 2015.
- [25] D Bernardi, E Pawlikowski, and John Newman. A general energy balance for battery systems. *Journal of the electrochemical society*, 132(1):5, 1985.
- [26] Matthew A Keyser. Battery thermal characterization. Technical report, National Renewable Energy Lab.(NREL), Golden, CO (United States), 2017.
- [27] Dong Zhang, Satadru Dey, Hector E Perez, and Scott J Moura. Real-time capacity estimation of lithium-ion batteries utilizing thermal dynamics. *IEEE Transactions on Control Systems Technology*, 28(3):992–1000, 2019.